Tetanus toxin is internalized by a sequential clathrin-dependent mechanism initiated within lipid microdomains and independent of epsin1

Katrin Deinhardt,[1] Otto Berninghausen,[2] Hugh J. Willison,[3] Colin R. Hopkins,[2] and Giampietro Schiavo[1]

[1]Molecular Neuropathobiology Laboratory, Cancer Research UK London Research Institute, London WC2A 3PX, England, UK
[2]Department of Biological Sciences, Imperial College London, London SW7 2AZ, England, UK
[3]Division of Clinical Neurosciences, Southern General Hospital, Glasgow G51 4TF, Scotland, UK

Ligand–receptor complexes are internalized by a variety of endocytic mechanisms. Some are initiated within clathrin-coated membranes, whereas others involve lipid microdomains of the plasma membrane. In neurons, where alternative targeting to short- or long-range trafficking routes underpins the differential processing of synaptic vesicle components and neurotrophin receptors, the mechanism giving access to the axonal retrograde pathway remains unknown. To investigate this sorting process, we examined the internalization of a tetanus neurotoxin fragment (TeNT H_C), which shares axonal carriers with neurotrophins and their receptors. Previous studies have shown that the TeNT H_C receptor, which comprises polysialogangliosides, resides in lipid microdomains. We demonstrate that TeNT H_C internalization also relies on a specialized clathrin-mediated pathway, which is independent of synaptic vesicle recycling. Moreover, unlike transferrin uptake, this AP-2–dependent process is independent of epsin1. These findings identify a pathway for TeNT, beginning with the binding to a lipid raft component (GD1b) and followed by dissociation from GD1b as the toxin internalizes via a clathrin-mediated mechanism using a specific subset of adaptor proteins.

Introduction

Endocytosis is essential for a variety of cellular functions, including the internalization of nutrients and communication among cells, or between cells and their environment. Internalized molecules must be precisely sorted to their final cellular destinations to fulfill their specific function. Distinct endocytic pathways have been described to date, including clathrin-dependent endocytosis and caveolae-mediated uptake, which remain the two best-characterized mechanisms of internalization (Conner et al., 2003). Neurons have adapted their endocytic pathways to better adjust to their specific requirements. Thus, synaptic vesicle (SV) recycling is the predominant form of neuronal endocytosis at the presynaptic terminal, whereby the fast fusion of neurotransmitter-containing vesicles is coordinated with an efficient mechanism of membrane recovery, which involves clathrin (for review see Murthy and De Camilli, 2003). In neurons, clathrin-independent routes have also been documented, although the physiological relevance of endocytosis via caveolae has been questioned in these cells because several of the caveolin isoforms found in other tissues are not detectable.

A special feature of motor neurons (MNs) is that their presynaptic terminal, which forms the neuromuscular junction (NMJ), is located in the periphery, whereas the soma is located in the central nervous system. Therefore, any material that enters the MNs at the NMJ and is transported toward the cell body, such as neurotrophins, crosses the blood–brain barrier. To gain more insights into the endocytic events at the NMJ, we followed the endocytosis of tetanus neurotoxin (TeNT). TeNT is a neurospecific toxin that binds to MNs at the NMJ, where it is internalized and undergoes axonal retrograde transport to the cell body. It is then secreted and taken up by adjacent inhibitory interneurons, where it blocks neurotransmitter release by cleaving VAMP/synaptobrevin, which is a synaptic SNARE (Lalli et al., 2003a).

K. Deinhardt and O. Berninghausen contributed equally to this work.

Correspondence to Giampietro Schiavo: Giampietro.Schiavo@cancer.org.uk

Abbreviations used in this paper: BoNT, botulinum neurotoxin; CCP, clathrin-coated pit; CCV, clathrin-coated vesicle; CHC, clathrin heavy chain; CLC, clathrin light chain; CTB, cholera toxin subunit B; DRM, detergent-resistant membrane; GPI, glycosylphosphatidylinositol; MESNA, 2-mercaptoethane sulfonic acid; MN, motor neuron; NMJ, neuromuscular junction; SV, synaptic vesicles; TeNT H_C, tetanus neurotoxin fragment.

The online version of this article contains supplemental material.

The Journal of Cell Biology, Vol. 174, No. 3, July 31, 2006 459–471
http://www.jcb.org/cgi/doi/10.1083/jcb.200508170

Supplemental Material can be found at:
http://www.jcb.org/cgi/content/full/jcb.200508170/DC1

The TeNT receptor complex has been shown to comprise lipids and proteins (Montecucco et al., 2004). The polysialogangliosides GD1b and GT1b (Habermann and Dreyer, 1986; Lalli et al., 2003a), as well as one or more glycosylphosphatidylinositol (GPI)-anchored proteins (Herreros et al., 2001; Munro et al., 2001) are required for toxin binding to the neuronal surface. TeNT is associated with detergent-resistant membranes (DRMs), which are enriched in cholesterol and GPI-anchored proteins (Herreros et al., 2001), and its uptake is sensitive to cholesterol depletion (Herreros et al., 2001). Furthermore, pretreatment of neurons with phosphatidylinositol-specific phospholipase C to cleave GPI-anchored proteins from their lipid anchor prevents TeNT intoxication (Munro et al., 2001). Altogether, these findings suggest that TeNT follows a polysialoganglioside- and DRM-dependent route for its internalization in neuronal cells. However, in previous EM studies on spinal cord neurons, gold-labeled TeNT was detected in surface pits resembling clathrin-coated invaginations, as well as in coated and uncoated vesicles (Parton et al., 1987; Lalli et al., 2003b). Because clathrin-mediated internalization and the endocytosis of proteins associated with DRMs have been largely viewed as mutually exclusive (Parton and Richards, 2003), the association of TeNT with clathrin coats was unexpected.

To resolve this apparent paradox, we have studied the internalization machinery responsible for the uptake of TeNT into MNs using a C-terminal binding fragment of TeNT (Lalli et al., 2003a). In this study, we show that TeNT H_C endocytosis in MNs is independent of SV recycling, the major route of internalization at the presynaptic terminal, and demonstrate that although TeNT H_C binds to DRMs on the MN surface, it uses a clathrin-mediated pathway for its entry. This specialized clathrin- and AP-2–dependent uptake mechanism does not require the endocytic adaptor protein epsin1, further indicating that specific adaptors play important functions in initial sorting events during endocytosis.

Results

TeNT H_C internalization in MNs is independent of presynaptic activity

Although previous studies implied that TeNT does not enter the NMJ via SV endocytosis (Habermann and Dreyer, 1986), some studies suggested that the toxin can take this route in brain-derived neurons, such as hippocampal neurons (Matteoli et al., 1996) and that it may enter SV-like vesicles in spinal cord neurons in culture (Parton et al., 1987). In light of these findings, we assessed whether SV exo/endocytosis is the physiological route of TeNT entry in MNs. Several lines of evidence indicate that this is not the case. First, we tested the colocalization of internalized TeNT H_C and the SV protein VAMP-2. MNs were incubated with Alexa Fluor 555–TeNT H_C at 37°C, fixed, and stained for VAMP-2. Under resting conditions, colocalization in the cell body, neurites, or synaptic contacts was very limited (Fig. 1, A and B). Moreover, stimulation of SV exo/endocytosis by depolarization did not increase the extent of colocalization (Fig. 1, A and B).

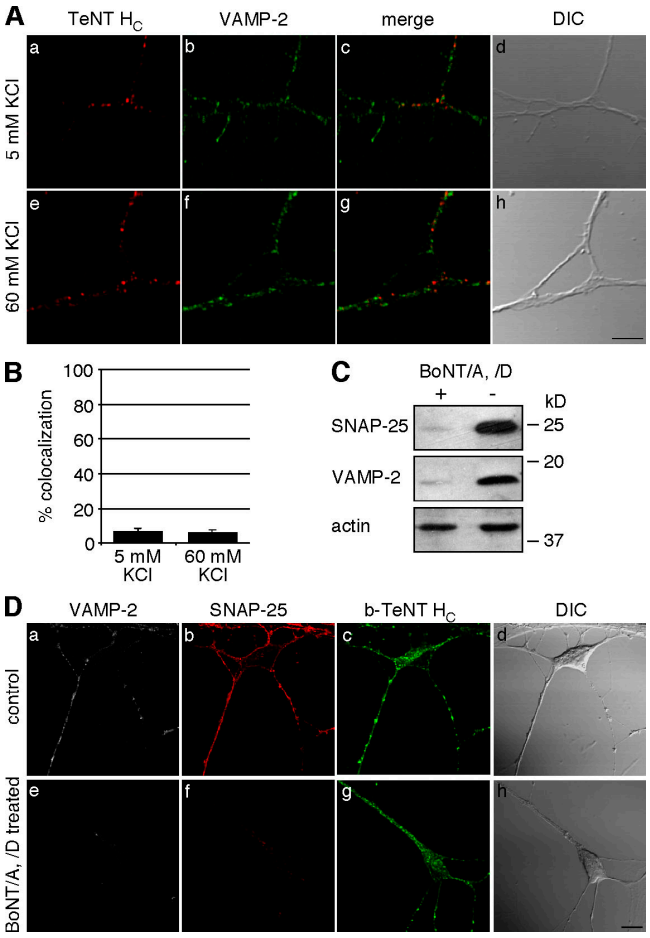

Figure 1. **TeNT H_C internalization is independent of SV exocytosis and recycling.** (A) MNs were incubated with 20 nM Alexa Fluor 555–TeNT H_C for 30 min at 37°C, either under resting conditions (a–d) or after stimulation of SV exo/endocytosis by adding 60 mM KCl to the medium just before TeNT H_C addition (e–h), fixed, and stained for VAMP-2. Only very limited colocalization of TeNT H_C and VAMP-2 under resting or stimulated conditions, which were quantified in B, was found. Error bars represent the SEM. (C and D) MNs were incubated with 15 nM BoNT/A and 2 nM BoNT/D for 22 h at 37°C to cleave SNAP-25 and VAMP-2. Untreated cells were processed in parallel for comparison. (C) Cells were scraped and analyzed by Western blotting using antibodies raised against the cleaved fragments of SNAP-25 and VAMP-2, as well as actin, as a loading control. (D) 20 nM b-TeNT H_C was added to MNs for 30 min at 37°C. MNs were shifted to ice, treated with MESNA before fixation, and stained for VAMP-2 (a and e), SNAP-25 (b and f), and biotin (c and g). Pretreatment with BoNTs did not affect TeNT H_C internalization. DIC, differential interference contrast. Bars: (A) 5 μm; (D) 10 μm.

To further investigate the endocytic pathway of TeNT, we used a biotinylated, thiol-cleavable form of TeNT H_C (b-TeNT H_C). By exposing intact neurons to cell-impermeable reducing reagents, such as 2-mercaptoethane sulfonic acid (MESNA; Schmid and Smythe, 1991), biotin can be cleaved off surface-bound TeNT H_C, while the internalized b-TeNT H_C is protected. Staining for the remaining biotin allows the internalized TeNT H_C to be detected selectively over the surface-bound TeNT H_C even in thin structures such as axons. Biotinylation does not change the binding and internalization properties of TeNT H_C because preincubation with a 100-fold excess of unlabeled toxin completely abolished the binding of b-TeNT H_C to MNs (Fig. S1 A, available at http://www.jcb.org/cgi/content/full/jcb.200508170/DC1). Furthermore, under internalization

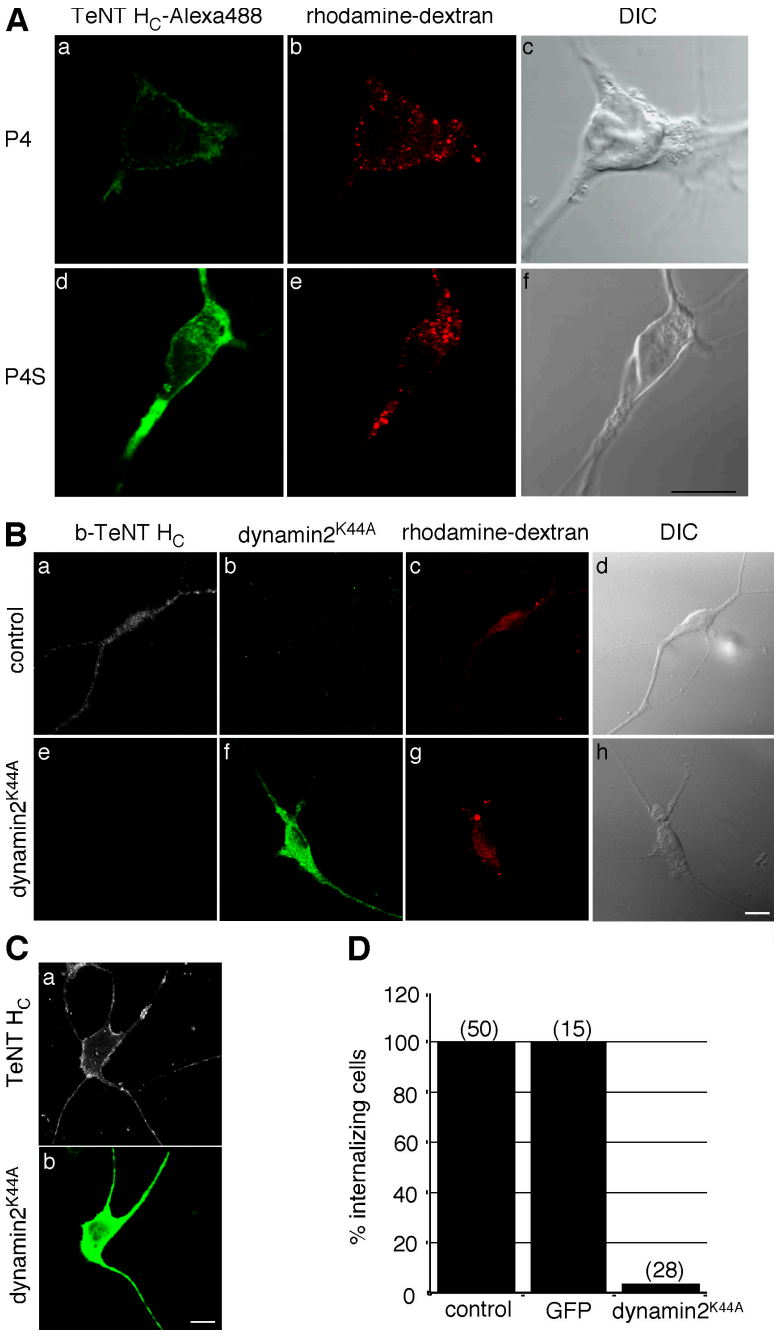

Figure 2. **Dynamin is required for TeNT H_C uptake into MNs.** (A) MNs were incubated with 50 μM of the cell-permeable peptide P4 (top) or its scrambled analogue P4S (bottom) for 2 h before addition of 20 nM Alexa Fluor 488–TeNT H_C and 0.2 mg/ml tetramethylrhodamine-dextran for additional 45 min. Images show confocal sections through the cell body. (B–D) MNs were microinjected with a plasmid encoding Myc-dynamin2^{K44A}. (B) After 25 h of expression, cells were incubated with 20 nM b-TeNT H_C and 0.2 mg/ml tetramethylrhodamine-dextran for 30 min at 37°C, treated with MESNA, fixed, stained for internal biotin and with an anti-Myc antibody to detect the tagged dynamin2^{K44A}, and imaged. (top) A control MN; (bottom) a microinjected cell. (C) Expression of dynamin2^{K44A} does not block the surface binding of TeNT H_C to MNs. 25 h after microinjection of dynamin2^{K44A}, MNs were incubated with Alexa Fluor 647–TeNT H_C for 30 min at 37°C, fixed, and stained with an anti-Myc antibody. A confocal section of an expressing cell is shown. (D) Quantitative analysis of the effect of dynamin2^{K44A} overexpression on TeNT H_C internalization. Noninjected MNs or cells microinjected with a GFP-encoding plasmid were taken as controls. Numbers in parenthesis indicate the number of MNs imaged per condition. DIC, differential interference contrast. Bars: (A) 5 μm; (B and C) 10 μm.

conditions, b-TeNT H_C colocalized with Alexa Fluor 555–TeNT H_C (Fig. S1 B). Importantly, biotin could be cleaved off the surface-bound b-TeNT H_C by treatment with MESNA on ice. In contrast, in cells incubated at 37°C the label remained cell-associated, showing that b-TeNT H_C had been taken up in the soma and neurites (Fig. S1 C).

For an independent assessment of a role for SV recycling in TeNT H_C uptake, we then preincubated MNs with botulinum neurotoxin (BoNT)/A and D for 22 h to block SV exocytosis, and, thus, recycling (Humeau et al., 2000). The samples were then incubated with b-TeNT H_C for 30 min at 37°C, treated with MESNA on ice, fixed, and stained for VAMP-2 and SNAP-25, as well as for biotin, to visualize internalized TeNT H_C. The complete cleavage of SNAP-25 and VAMP-2 by BoNT/A and D was confirmed by Western blotting (Fig. 1 C) and by indirect immunofluorescence (Fig. 1 D), indicating that SV exo/endocytosis was blocked under these conditions. However, TeNT H_C internalization was not affected in intoxicated MNs (Fig. 1 D, g) compared with untreated cells (Fig. 1 D, c).

TeNT H_C uptake is dynamin-dependent

We next used the b-TeNT H_C to test the requirement for dynamin in this process. Dynamin is a GTPase essential for clathrin- and caveolin-mediated endocytosis, as well as for several other endocytic and vesicle-trafficking events. Incubation of MNs with the cell-permeable peptide P4, which inhibits dynamin function (Marks and McMahon, 1998), but not with the scrambled

peptide P4S, significantly reduced uptake of TeNT H_C, whereas its overall binding to the neuronal surface was not affected (Fig. 2 A). These results were confirmed by overexpressing the well-characterized dynamin mutant K44A, which is defective in GTP binding and hydrolysis and restrains invaginated pits from pinching off (Fig. 2 B; Damke et al., 1994). We used microinjection to introduce foreign DNA into MNs because lipid-based transfection reagents abolished axonal transport in MNs. In contrast, microinjection of plasmids driving the overexpression of control proteins had no effect on cell viability and retrograde transport (Deinhardt and Schiavo, 2005). Expression of dynamin2^{K44A} significantly reduced TeNT H_C endocytosis at the level of both the soma and neurites (Fig. 2 B), without affecting its binding to the MN surface (Fig. 2 C). These results indicate that dynamin is a central player in TeNT H_C internalization and rule out differences in the mechanism of uptake of TeNT H_C between axons and the soma. This is important because, topologically, only the axon is physiologically relevant for TeNT H_C uptake and retrograde transport. A total block of TeNT H_C endocytosis by the expression of dynamin2^{K44A} was seen in >95% of the cells (Fig. 2 D). However, dextran internalization still took place under these conditions (Fig. 2 B, g) or upon P4 treatment (Fig. 2 A, b), confirming that MNs were viable and still capable of endocytosis via dynamin-independent pathways. We chose dextran as a control marker for internalization because we found that cholera toxin subunit B (CTB), which is another widely used marker for clathrin-independent endocytosis, is internalized in a strictly dynamin-dependent fashion in MNs (unpublished data). This was surprising because CTB has been shown to use a dynamin-independent entry pathway in other cell types, such as HeLa and mouse embryonic fibroblasts (Torgersen et al., 2001; Massol et al., 2004; Kirkham et al., 2005; Glebov et al., 2006).

TeNT H_C localizes to clathrin-coated pits

In previous studies, TeNT was found in coated pits, as well as in coated and uncoated vesicles in spinal cord neurons (Parton et al., 1987; Lalli et al., 2003b). Furthermore, TeNT is taken up by a clathrin-independent route in nonneuronal cells (Montesano et al., 1982). Therefore, we decided to investigate whether TeNT internalization is strictly clathrin-mediated in cultured MNs. First, we assessed the colocalization of clathrin and TeNT H_C at the light microscopy level in MNs microinjected with GFP–clathrin light chain (CLC). Upon incubation with TeNT H_C at 37°C, we could see only a partial overlap between GFP-CLC and TeNT H_C, more readily in the cell body than in the axon (Fig. 3, A and B).

To verify this colocalization at a fine structural level, we used TeNT H_C coupled with HRP. Just like b-TeNT H_C, binding of this fusion protein to MNs was inhibited by preincubation with an excess of unlabeled TeNT H_C and, upon internalization, Alexa Fluor 488–TeNT H_C and HRP–TeNT H_C showed extensive colocalization (Fig. S2, A and B, available at http://www.jcb.org/cgi/content/full/jcb.200508170/DC1). The relationship between internalized TeNT H_C and clathrin-coated structures was then investigated at early stages of the internalization process. To this end, we synchronized the uptake of HRP–TeNT H_C by preincubating the MNs at 4°C and, subsequently, warming to 12°C. This low-temperature treatment allows the plasma membrane to invaginate but inhibits vesicle–pinching off (unpublished data). The effectiveness of this protocol was

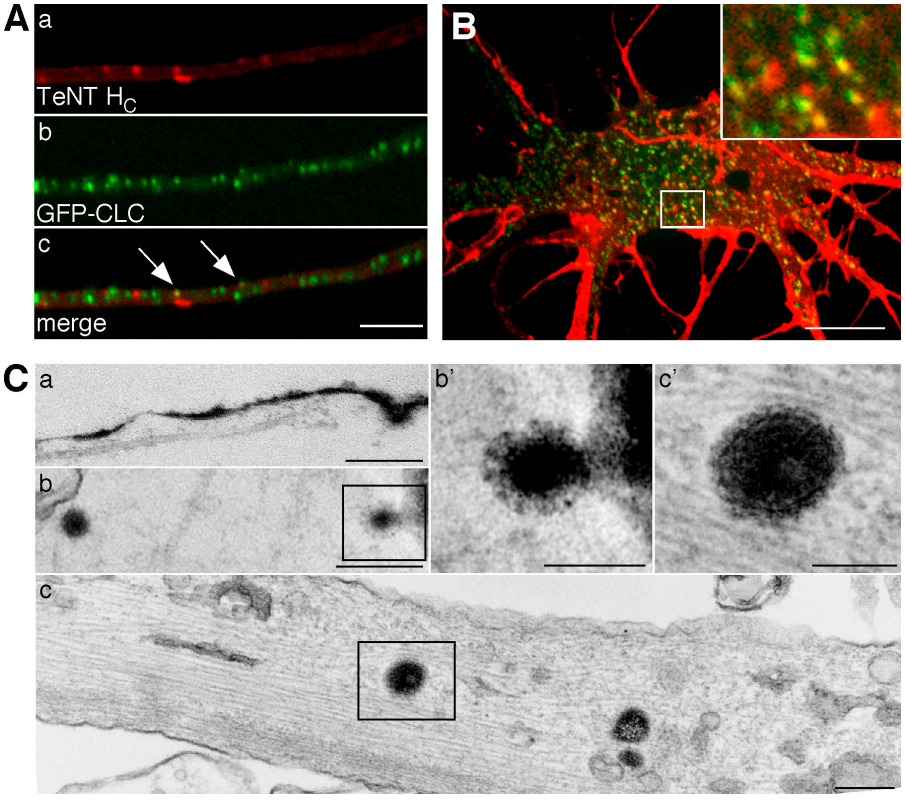

Figure 3. **TeNT H_C enters clathrin-coated structures in MNs.** (A and B) MNs were microinjected with a plasmid encoding GFP-CLC. After overnight expression, cells were incubated with 30 nM Alexa Fluor 555–TeNT H_C, washed, and imaged. (A) GFP-CLC and TeNT H_C dual-positive structures are visible in an axon (arrows). (B) Confocal section of the bottom plane of a MN soma. A partial overlap between GFP-CLC–positive and TeNT H_C–positive structures is observed (inset). (C) MNs were incubated with HRP–TeNT H_C for 45 min on ice, and then chased for 45 min at 12 (a and b) or 18°C (c). Cells were fixed and incubated with DAB/H_2O_2 to label HRP–TeNT H_C. The electron-dense DAB reaction product was often associated with coated pits and budding vesicles, which were visible at higher magnification (b′ and c′). Bars: (A) 2 μm; (B) 5 μm; (C) 0.2 μm.

confirmed by incubating MNs with either b-TeNT H_C or HRP–TeNT H_C at 12°C and, subsequently, treating cells with MESNA or performing the DAB reaction in the presence of ascorbic acid, which is a membrane-impermeable inhibitor of the HRP staining (Stoorvogel, 1998). Upon MESNA treatment, no biotin was detectable by immunofluorescence (Fig. S2 C). Similarly, when the DAB reaction was performed in the presence of ascorbic acid on cells incubated at 12°C, we observed immunolabeling of clathrin, but no DAB staining (Fig. S2 D). These findings indicated that the coated pits remained open to the external medium at 12°C and confirmed the suitability of this temperature block for the study of the initial stages of endocytosis.

After 12°C incubations, the electron-dense DAB reaction product generated by HRP–TeNT H_C was readily observed in coated pits on the plasma membrane of soma, dendrites, and axons (Fig. 3 C). The nature of these coated domains was confirmed by immunogold staining with clathrin heavy chain (CHC) antibodies, which labeled pits containing HRP–TeNT H_C (Fig. 4 A). The DAB reaction product found in both shallow pits and in deeper invaginations was closely associated with clathrin lattice components (Fig. 3 C, a–b'). After the 12°C block, we allowed MNs to internalize TeNT H_C at 18°C to monitor its intracellular axonal transport. Fine structural analysis suggests that progression along the endocytic pathway was slowed down at this temperature and lead to an increase of early endosomal carriers. At 18°C, HRP–TeNT H_C was found in coated vesicles (Fig. 3 C, c) and other vesicular and tubular structures within the axon.

Gold immunolabeling of coated pits in axons was not easily discerned in thin EM sections, as permeabilization of these structures and access to the antigen appeared to be impaired because of the highly packed cytoskeleton in these areas. Therefore, we decided to prepare whole-cell mounts by extracting neurons with Triton X-100 before fixation, thereby improving the antigen availability and providing a better overview over the total population of TeNT H_C–positive membranes. To stabilize HRP–TeNT H_C–containing pits and protect them from solubilization, DAB cross-linking was performed before detergent extraction. At 12°C, the vast majority of DAB-positive structures located along the axons (Fig. 4 B, a, b, and d) and on the cell body (Fig. 4 B, c) were clathrin positive.

The ganglioside GD1b does not enter coated pits in complex with TeNT H_C

Polysialogangliosides of the b-series, including GD1b and its analogues GT1b and GQ1b, have previously been described as

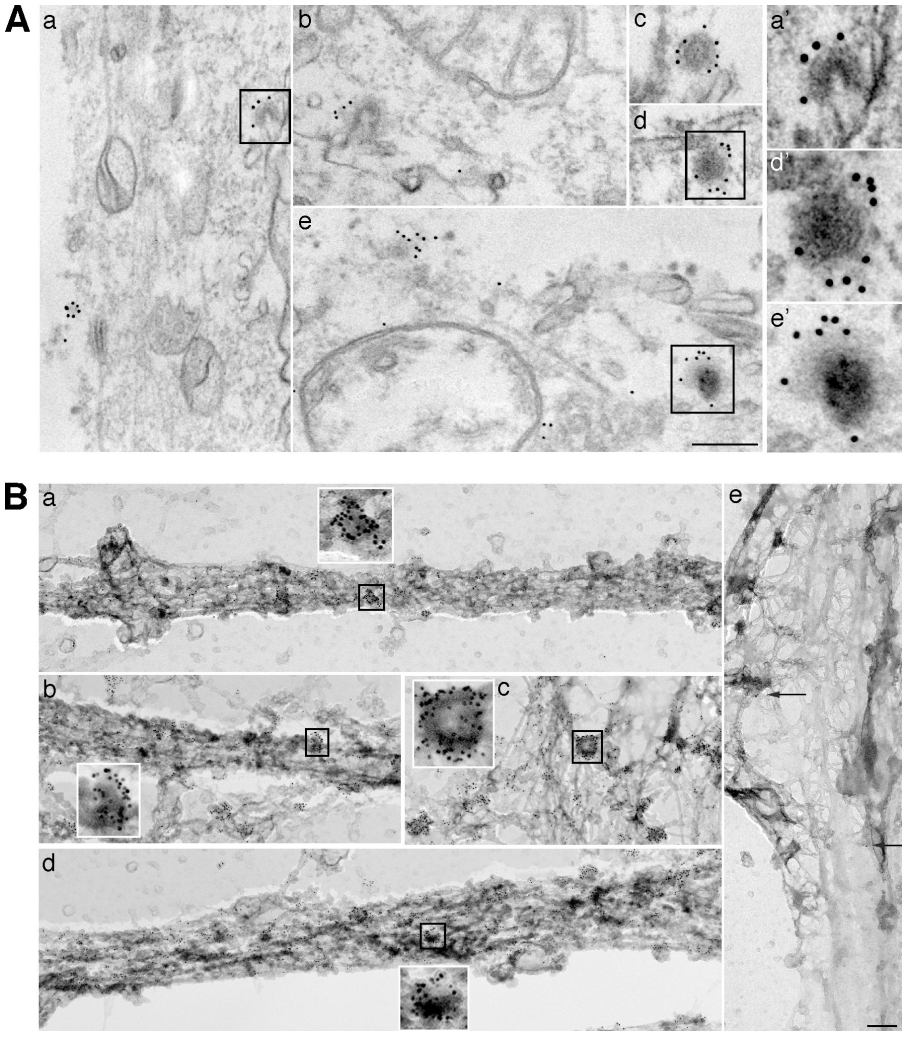

Figure 4. **Colocalization of HRP–TeNT H_C and clathrin at EM level.** (A) HRP–TeNT H_C–containing structures are labeled with anti-CHC. Cells were loaded with HRP–TeNT H_C at 12°C for 45 min before HRP cross-linking with DAB/H_2O_2. MNs were permeabilized with digitonin before labeling with an anti-CHC antibody and incubated with a rabbit anti–mouse bridging antibody, and then with 10 nm immunogold. (B) Whole-mount transmission EM showing distribution of clathrin in vesicles loaded with HRP–TeNT H_C. (a–d) MNs were incubated with HRP–TeNT H_C at 12°C for 45 min, cross-linked with DAB/H_2O_2, extracted with Triton X-100, and then treated with an anti-CHC antibody followed by a bridging antibody and 10 nm immunogold. HRP–TeNT H_C is found in CCPs and CCVs in axons (a, b, d) and soma (c). Control without the bridging antibody showed negligible labeling (e, arrows). Boxed areas show enlarged examples of TENT H_C–positive endocytic structures. Bars, 0.2 μm.

essential components of the TeNT receptor complex (Kitamura et al., 1999). However, these lipids, like other residents of sphingolipid-rich microdomains, are thought not to enter clathrin-coated pits (CCPs; Nichols, 2003). Therefore, we asked where GD1b localizes on the neuronal surface in relation to TeNT H_C and clathrin-coated invaginations. By light microscopy, we were able to confirm colocalization of TeNT H_C and GD1b on the neuronal surface by using a specific anti- GD1b antibody (MOG-1; Fig. 5 A). Furthermore, preincubation of MNs with MOG-1 inhibited the binding of TeNT H_C in a dose-dependent manner (Fig. S3 A, available at http://www.jcb.org/cgi/content/full/jcb.200508170/DC1), confirming that GD1b is an essential component of the TeNT receptor complex. To obtain a higher resolution view of the association between TeNT H_C and polysialogangliosides, we incubated MNs with HRP–TeNT H_C in the presence of noncompeting concentrations of MOG-1 at 12°C (Fig. S3 B) and analyzed the samples by EM. As previously described for other components of lipid microdomains, we found clusters of gold-labeled GD1b on the cell surface, often in close proximity to the DAB precipitate generated by HRP–TeNT H_C (Fig. 5 B). In addition, the DAB precipitate was frequently associated with coated structures (Fig. 5 B, arrows and arrowheads). However, we were unable to detect GD1b in CCPs containing the DAB cross-linking product. Instead, gold-labeled GD1b

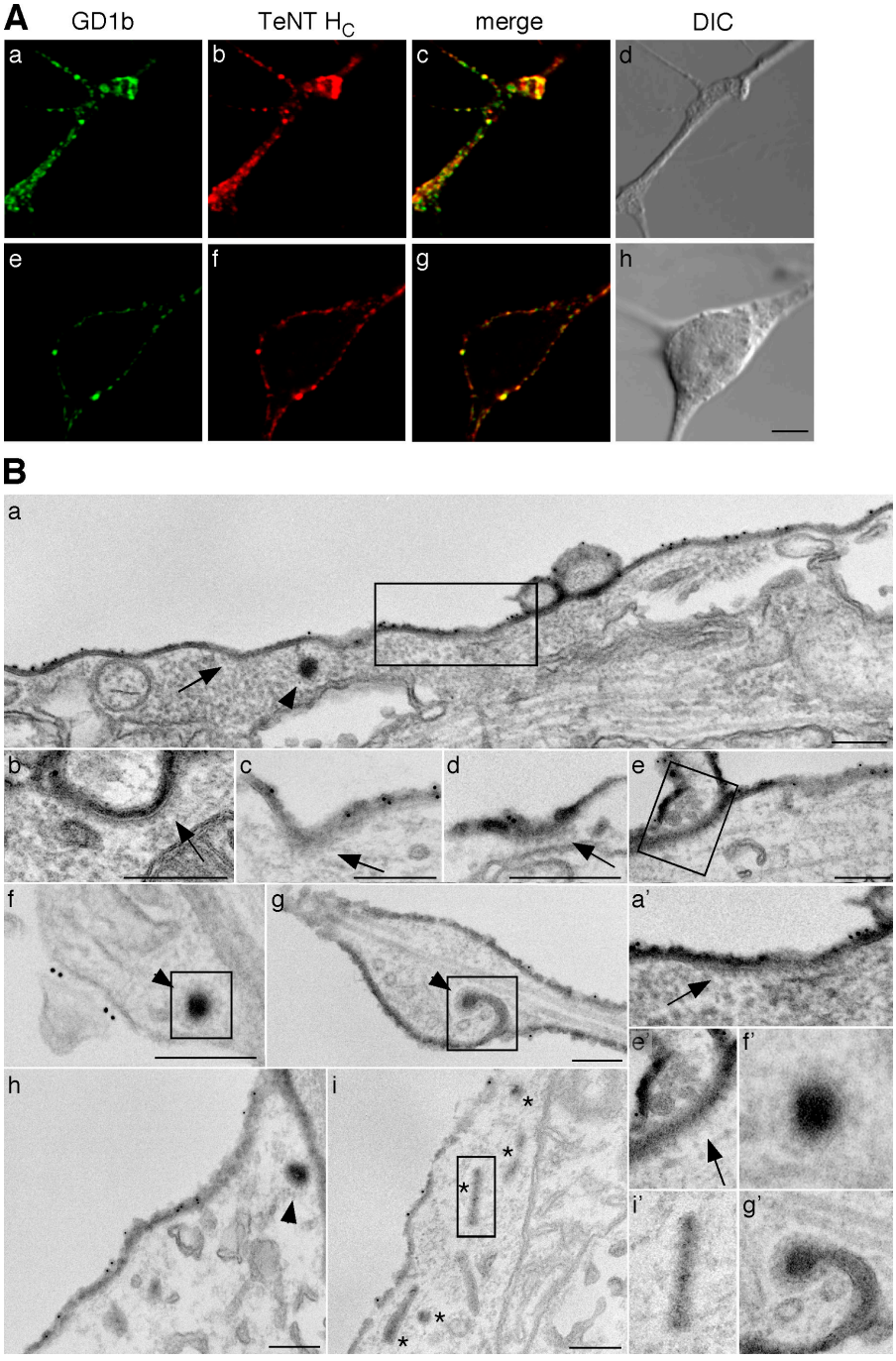

Figure 5. **GD1b and TeNT H_C undergo independent sorting on the plasma membrane.** MNs were probed with TeNT H_C and an anti-GD1b antibody and analyzed at light and EM levels. (A) Cells were incubated with the antibody MOG-1 (2 μg/ml) and 20 nM Alexa Fluor 555–TeNT H_C for 30 min on ice, followed by 5 min at 22°C, and then were washed, fixed, and imaged. A good overlap of the two signals could be seen both on neurites (a–d) and soma (e–h). DIC, differential interference contrast. (B) EM analysis. MNs were incubated on ice with 60 nM HRP–TeNT H_C and 10 μg/ml MOG-1, followed by 10 nm immunogold. After washing, samples were shifted to 12°C for 45 min (a–h) or 37°C for 15 min (i). MNs were fixed and incubated with DAB/H_2O_2 to label HRP–TeNT H_C. The anti-GD1b gold-labeled antibody is excluded from endocytosed HRP–TeNT H_C vesicles (asterisks), clathrin lattices (arrows), and invaginated coated pits (arrowheads). Bars, 0.2 μm.

was frequently found at the edge of HRP–TeNT H_C–positive pits (Fig. 5 B, a–h). Furthermore, internalized gold particles were very rarely detected upon incubation at 37°C, suggesting that GD1b remains surface-bound (Fig. 5 B, i). Under the same conditions, TeNT H_C was identifiable in many vesicles and tubules, all of which were free of GD1b gold label (Fig. 5 B, i). To confirm that the DAB precipitate did not conceal any gold particles in internalized structures, we incubated MNs with HRP–TeNT H_C together with gold-conjugated TeNT H_C. Under these conditions, gold label was clearly visible in all HRP-positive structures (Fig. S2 E).

A subset of clathrin endocytic adaptors is required for TeNT H_C endocytosis

We next examined whether CCP formation is required for TeNT H_C internalization by affecting specific components of the clathrin-dependent endocytic machinery. The blockade of transferrin uptake, which strictly relies on a clathrin-mediated pathway (Harding et al., 1983), was taken as a positive control, whereas the CTB entry, which occurs via clathrin-independent routes in several cell types (Torgersen et al., 2001; Nichols, 2003; Kirkham et al., 2005), allowed us to monitor the specificity of the inhibition. In control MNs, both CTB and b-TeNT H_C readily entered neurons in soma and neurites (Fig. 6, a and c). Expression of the phosphorylation-deficient mutant of the AP-2 subunit μ2 ($\mu2^{T156A}$), which is incorporated into AP-2 complexes but cannot be phosphorylated at Thr156, thus, impairing AP-2–dependent clathrin-mediated endocytosis (Olusanya et al., 2001), blocked the uptake of TeNT H_C (Fig. 6 d), as well as transferrin internalization (not depicted). In contrast, CTB entry in $\mu2^{T156A}$-expressing MNs is barely altered (Fig. 6 f), suggesting that, in contrast to that observed in hippocampal neurons (Shogomori and Futerman, 2001), its mechanism of uptake in MNs is mainly clathrin independent. As expected, binding of TeNT H_C to the cell surface was not affected by expression of $\mu2^{T156A}$ (not depicted). Similar results were obtained by expressing a truncation mutant of the accessory protein AP180 (AP180-C). This mutant inhibits uptake of EGF and transferrin in COS-7 cells (Ford et al., 2001). Expression of AP180-C inhibited both TeNT H_C (Fig. 6 g) and transferrin endocytosis (not depicted), whereas CTB internalization was not visibly affected (Fig. 6 i).

In contrast to AP-2 and AP180 dominant-negative constructs, expression of a mutant version of the adaptor protein epsin1 had no significant effect on TeNT H_C internalization (Fig. 7 A, d and g). This epsin1$^{R63L\ H73L}$ mutant is unable to bind phosphatidylinositol-4,5-bisphosphate (PtdIns[4,5]P_2) and blocks transferrin uptake in COS-7 cells (Ford et al., 2002). As expected, transferrin endocytosis was completely inhibited in epsin1$^{R63L\ H73L}$-expressing MNs (Fig. 7 A, f). These findings were confirmed by an independent EM analysis, where expression of this epsin1 mutant abolished the uptake of transferrin-HRP (not depicted), leaving the internalization of HRP–TeNT H_C unaffected (Fig. 7 B, arrows). In addition, epsin1$^{R63L\ H73L}$-expressing cells showed no obvious morphological alterations and displayed occasional CCPs and clathrin-coated vesicles (CCVs; Fig. 7 B, arrowheads and insets). These findings, together with previous works reporting the existence of AP-2–independent

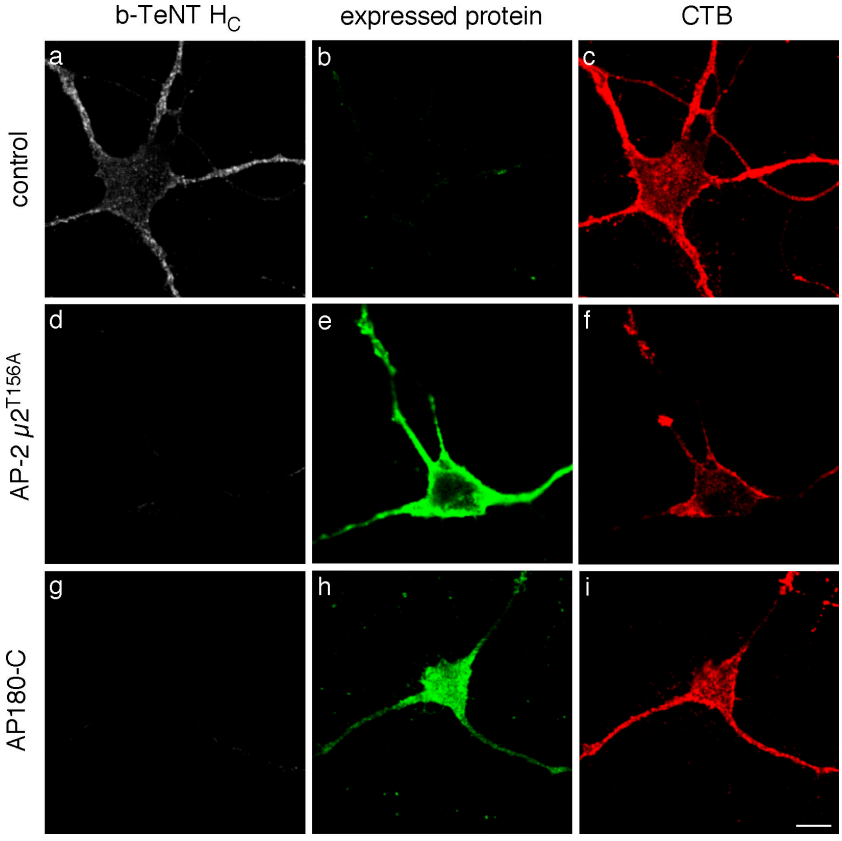

Figure 6. **Internalization of TeNT H_C is dependent on a functional clathrin machinery.** 25 h after microinjection of the AP-2 $\mu2^{T156A}$ and tTA plasmids (d–f), or 26 h after microinjection of a plasmid encoding AP180-C (g–i), MNs were incubated with 20 nM b-TeNT H_C and 10 ng/ml Alexa Fluor 555–CTB for 30 min, MESNA-treated, fixed, stained for internal biotin and the epitope tags of the microinjected constructs, and imaged. (a–c) Uninjected MNs were imaged as a control. Bar, 10 μm.

routes (Nesterov et al., 1999; Conner and Schmid, 2003; Hinrichsen et al., 2003; Motley et al., 2003; Lakadamyali et al., 2006), suggest that different subsets of adaptors proteins functionally define distinct clathrin-dependent pathways.

To investigate the spatial relationships of TeNT H_C, transferrin, and epsin1 during the early stages of endocytosis, we analyzed the distribution of epsin1 by immuno-EM in MNs incubated with gold-conjugated TeNT H_C and transferrin-HRP at 12 or 20°C. Under these conditions, we could detect TeNT H_C in clathrin-coated structures either containing or devoid of transferrin, as well as transferrin-containing pits and vesicles devoid of TeNT H_C (Fig. S4 A, available at http://www.jcb.org/cgi/content/full/jcb.200508170/DC1). Quantitative analysis of all TeNT H_C–containing structures revealed that 54% of these were devoid of transferrin. Interestingly, less than half of these TeNT H_C single-positive structures labeled for epsin1, whereas two-thirds of the TeNT H_C and transferrin dual-positive vesicles and pits were also positive for epsin1 (Fig. S4 B). Therefore, epsin1 accumulates preferentially, but not exclusively, on transferrin-containing structures. It should be considered, however, that permeabilization with digitonin is likely to affect the stability of HRP-negative membranes (TeNT H_C ± epsin1). Therefore, these structures are likely to be underestimated, as observed by independent experiments in which the occurrence of transferrin-HRP and HRP– TeNT H_C containing CCP and CCV has been quantified (unpublished data).

The effects of the disruption of different components of the clathrin-dependent machinery on TeNT H_C uptake are evident in the quantitative analysis provided in Fig. 7 C. Although TeNT H_C endocytosis into MNs can be blocked by disruption of the

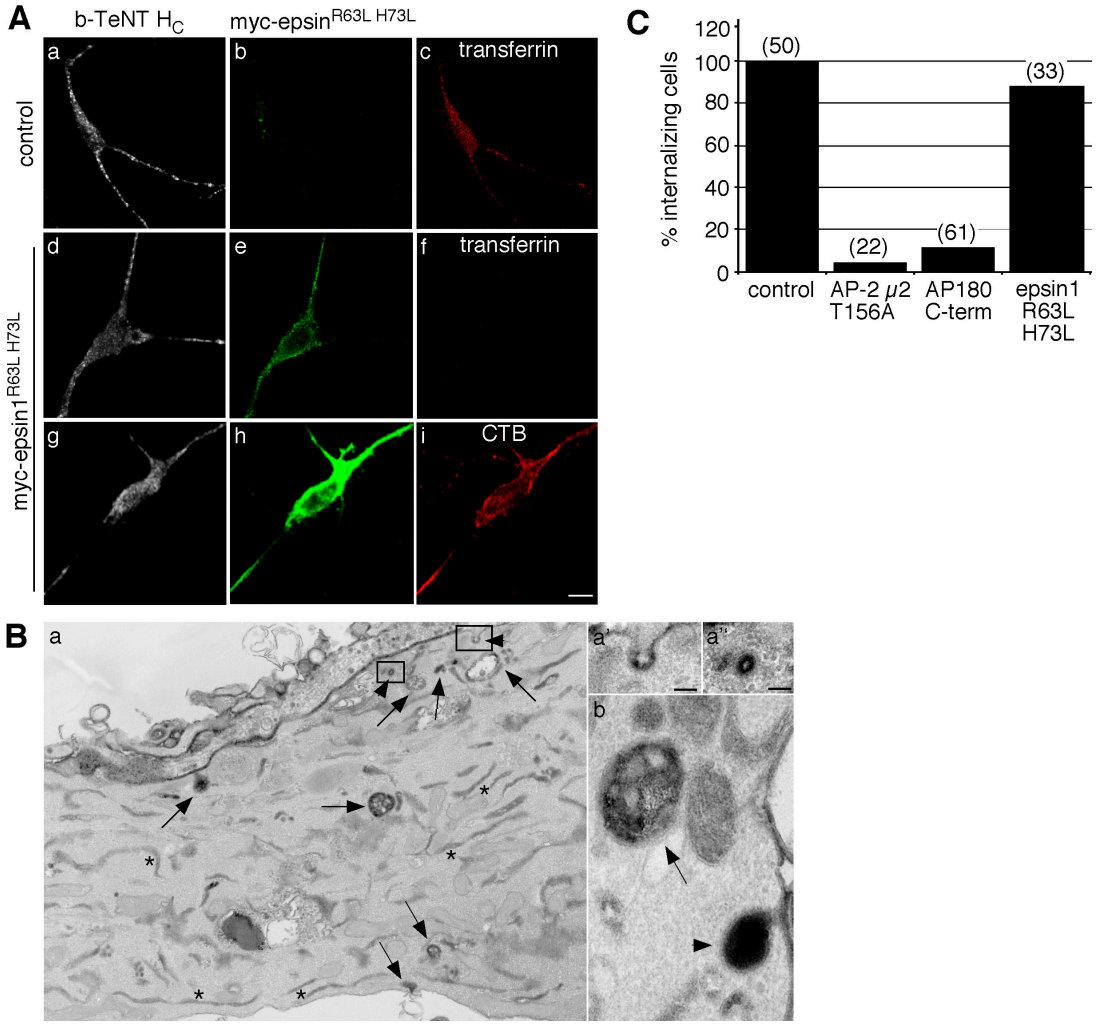

Figure 7. **TeNT H_C endocytosis is independent of epsin1.** MNs were microinjected with a plasmid encoding epsin1$^{R63L\ H73L}$. (A) After 26 h, cells were incubated with 20 nM b-TeNT H_C and 20 μg/ml Alexa Fluor 594–transferrin or 10 ng/ml Alexa Fluor 555–CTB for 30 min at 37°C and then shifted on ice for MESNA treatment. MNs were fixed and stained for internal biotin and with an anti-Myc antibody before imaging. Control cells readily internalized both transferrin and TeNT H_C (a–c), whereas transferrin, but not TeNT H_C uptake was blocked in microinjected cells (d, f, and g). CTB internalization was also not affected in epsin1$^{R63L\ H73L}$-expressing cells (i). (B) 26 h after comicroinjection with plasmids encoding epsin1$^{R63L\ H73L}$ and HRP-KDEL, MNs were incubated with HRP–TeNT H_C for 30 min at 37°C. Cells were then treated with DAB/H_2O_2 and analyzed by EM. Transfection was confirmed by the characteristic DAB staining of the tubular ER (asterisks). The DAB reaction product generated by HRP–TeNT H_C was found in various endosomes, multivesicular body–like structures (arrows), and in CCVs (arrowheads and insets). (C) Quantification of the effects of the overexpression of dominant-negative mutants on TeNT H_C endocytosis as determined in Fig. 5 and Fig. 6 A. Numbers in parenthesis indicate the number of MNs observed per condition. Bars: (A) 10 μm; (B) 0.2 μm.

clathrin adaptors AP-2 and AP180, it does not require the adaptor protein epsin1. Given that epsin1 is targeting ubiquitinated receptors to the late endosomal/lysosomal pathway (Le Roy and Wrana, 2005), the independence of TeNT H_C internalization from epsin1 function is in agreement with the finding that TeNT H_C escapes targeting to acidic compartments and degradation in MNs (Lalli et al., 2003a; Bohnert and Schiavo, 2005).

Discussion

An open question in the field of membrane trafficking is how distinct extracellular ligands following internalization via the same endocytic pathway (i.e., CCPs, caveolae), are sorted in early endosomes to their different intracellular destinations. In neurons, this process is crucial for the targeting of growth factors and their receptor complexes to short- and long-range trafficking routes, ultimately leading to diverse and often opposite biological functions. This is exemplified by the action of nerve growth factor, which has been shown to alter growth cone dynamics by local signaling, while it acts as a survival factor following axonal retrograde transport and transcriptional activation in the nucleus (Miller and Kaplan, 2001). The fine balance between these two processes is fundamental for our understanding of differentiation, synaptogenesis, and plasticity in the nervous system.

TeNT H_C was chosen as a tool to monitor endocytosis in MNs based on its high binding affinity to neuronal membranes (Lalli et al., 2003a) and its ability to enter the same axonal transport compartment used by nerve growth factor (Lalli and Schiavo, 2002) and the neurotrophin receptor $p75^{NTR}$ (unpublished data). Previous work highlighted the association of TeNT with both coated and uncoated structures, whereas at later time points it was found in many endocytic organelles, including coated and uncoated vesicles, tubules, and SV-like profiles (Montesano et al., 1982; Parton et al., 1987; Matteoli et al., 1996; Miana-Mena et al., 2002; Lalli et al., 2003b; Roux et al., 2005). However, a functional analysis assessing the role of the various internalization routes has yet to be made.

We show that clathrin-dependent internalization plays a nonredundant role in the uptake of TeNT in MNs. At 37°C, CCPs and CCVs that are positive for TeNT are rarely found, especially along axons. To explore if the localization to coated structures is representative for the entire TeNT H_C pool, we lowered the temperature to inhibit fission, thus, trapping forming pits on the cell surface. A striking colabeling of TeNT H_C and clathrin was seen under these conditions. Importantly, whole-mount EM analysis revealed that the HRP–TeNT H_C–containing areas along the axon were positive for clathrin, indicating that TeNT H_C does enter MNs via CCPs. In this light, the uncoated structures containing TeNT H_C observed previously (Schwab and Thoenen, 1978; Parton et al., 1987; Lalli et al., 2003b) may represent vesicles from which the clathrin lattice was rapidly removed (Blanpied et al., 2002; Ehrlich et al., 2004).

Several virulence factors, such as cholera and Shiga toxins, are taken up by clathrin-dependent and -independent routes (Sandvig and van Deurs, 2002; Parton and Richards, 2003; Saint-Pol et al., 2004), which may display different extents of cross talk and redundancy in various cell types (Torgersen et al., 2001). To ensure that clathrin-dependent endocytosis is the main, nonredundant route of TeNT H_C internalization and identify the endocytic machinery responsible for its uptake, we used dominant-negative constructs interfering with distinct steps of coat recruitment and/or pinching off from the plasma membrane. Impairing dynamin function led to a block in TeNT H_C uptake, showing that this GTPase is necessary for TeNT H_C endocytosis. In addition, disruption of the clathrin machinery by mutants of AP180 nearly completely abolished TeNT H_C internalization. Furthermore, the uptake of TeNT H_C, as well as of transferrin in MNs, are strictly AP-2–dependent, confirming previous findings obtained with transferrin in other cell types (Hinrichsen et al., 2003; Motley et al., 2003; Lakadamyali et al., 2006). Thus, a functional clathrin machinery is strictly required for TeNT H_C endocytosis (Fig. 8).

In contrast, expression of a dominant-negative epsin1 mutant did not interfere with TeNT H_C internalization. Epsin1 is an endocytic adaptor for clathrin-dependent and -independent internalization that binds to ubiquitinated receptors via its ubiquitin interacting motifs (Chen and De Camilli, 2005; Le Roy and Wrana, 2005; Sigismund et al., 2005). It has a modular structure comprising binding sites for PtdIns(4,5)P_2, CHC, AP-2, and other accessory factors for clathrin-mediated endocytosis. The mutant used in our study is deficient in PtdIns(4,5)P_2 binding (Ford et al., 2002) and was reported to block endocytosis by sequestering AP-2. However, we observed opposite effects with the AP-2 μ2 and the epsin1 mutants on TeNT H_C uptake in MNs, suggesting that their inhibitory activity may not completely overlap. In contrast with that reported in COS-7 cells, we did not detect aggregation of AP-2 in MNs or glial cells expressing $epsin1^{R63L\ H73L}$ (Fig. S5, available at http://www.jcb.org/cgi/content/full/jcb.200508170/DC1). In these conditions, uptake of transferrin into MNs was blocked by expression of this epsin1 mutant, indicating that $epsin1^{R63L\ H73L}$ displays a dominant-negative effect in these cells that is likely to be independent of AP-2 sequestration.

Epsin1 function overlaps with that of the homologues Eps15 or Eps15R, as shown by the limited effect of single and double knockdown on transferrin and EGF internalization in HeLa cells (Huang et al., 2004). In contrast, transferrin uptake was completely blocked by expression of $epsin1^{R63L\ H73L}$, demonstrating that epsin1 has a nonredundant function in a subset of clathrin-mediated, AP-2–dependent endocytic events in MNs (Fig. 8). Moreover, the block of transferrin internalization by $epsin1^{R63L\ H73L}$ suggests that epsin1 acts at an early step of the uptake process, before pit closure, implying that sorting in the endocytic pathway initiates at the plasma membrane. In this regard, we found epsin1 to be associated preferentially, but not exclusively, with transferrin-containing CCPs and CCVs. In agreement with this view, the sorting of endocytic cargoes internalized via clathrin-mediated uptake, such as low- density lipoprotein and influenza virus, to distinct population of endosomes has been shown to begin at the level of CCPs (Lakadamyali et al., 2006).

In spite of its entry into MNs via a clathrin-dependent mechanism, TeNT H_C binds to DRMs, and its uptake can be

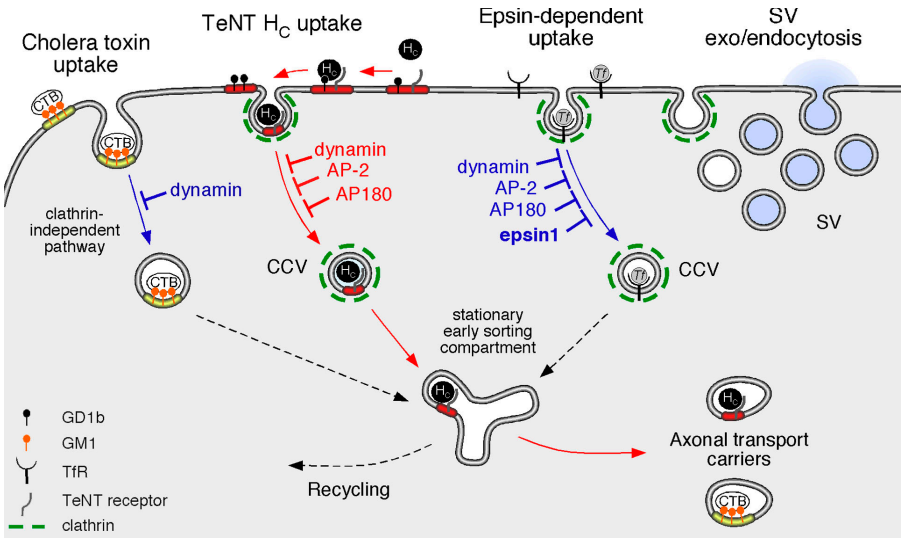

Figure 8. **Internalization pathways in MNs.** Transferrin uptake is mediated by a classical clathrin-dependent internalization route occurring in soma and dendrites. SV exo/endocytosis accounts for the majority of endocytic events at the presynaptic terminal and may involve multiple clathrin-dependent steps. In contrast, CTB, which binds to GM1 clustered in lipid rafts, is internalized by a clathrin-independent, dynamin-dependent mechanism in MNs. TeNT H_C exploits a pathway requiring lipid rafts and the clathrin machinery, which is distinct from aforementioned routes of internalization. At the NMJ, TeNT H_C binds to a lipid–protein receptor complex containing the ganglioside GD1b. TeNT H_C is then laterally sorted into CCPs and, during this sorting event, GD1b is excluded from the toxin receptor complex. Internalization of TeNT H_C is dependent on dynamin, AP-2, and AP180, but does not require epsin1. Once internalized, TeNT H_C is targeted to a stationary early sorting compartment (Lakadamyali et al., 2006), to which other endocytic routes may converge. This early sorting compartment is functionally coupled to the axonal retrograde transport pathway.

blocked by cholesterol sequestration and cleavage of GPI-anchored proteins (Herreros et al., 2001; Munro et al., 2001). Therefore, TeNT H_C may use endocytic mechanisms that have, until recently, been viewed as mutually exclusive. Some components of DRMs, such as GM1, are excluded from CCPs (Nichols, 2003); others do not require a functional clathrin machinery or dynamin for their internalization (Lamaze et al., 2001; Sabharanjak et al., 2002; Le Roy and Wrana, 2005). However, evidence suggesting an overlap between these two endocytic routes has been recently reported in the case of anthrax toxin (Abrami et al., 2003), chemokine receptor 5 (Venkatesan et al., 2003; Signoret et al., 2005), and prion protein (Sunyach et al., 2003). In light of these findings, it is clearly of interest to determine if TeNT H_C, on recruitment to DRMs, remains within its lipid environment during internalization or is transferred to a modified receptor complex before sorting into CCP. To address this issue, we examined the spatial relationship between TeNT H_C, coated pits, and GD1b. Although we readily observed TeNT H_C and GD1b clustered together at the neuronal surface, we were unable to detect GD1b within CCP. Interestingly, GD1b-associated immunogold was frequently found at the edge of TeNT H_C–positive pits. These observations suggest that even though GD1b and other b-series gangliosides are essential for TeNT binding to the neuronal surface and toxicity (Kitamura et al., 1999), TeNT H_C is no longer in complex with the bulk of GD1b during internalization. This hypothesis is strengthened by the lack of internalization of the anti-GD1b antibody over the time intervals used in our experiments (unpublished data) and the slow kinetics of retrograde transport of gangliosides in vivo (Aquino et al., 1985). In this model, TeNT H_C is initially captured by GD1b microdomains before being targeted to CCP (Fig. 8). This lateral sorting, which could require the integrity of lipid rafts (Herreros et al., 2001), might be mediated by glycosylated proteins binding the carbohydrate-binding pockets of TeNT H_C that were previously occupied by GD1b or other b-series gangliosides (Rummel et al., 2003). CTB instead binds to GM1-enriched lipid rafts on the plasma membrane, leading to its internalization via a clathrin-independent, dynamin-dependent pathway in MNs and its late appearance in axonal carriers distinct from those containing TeNT H_C (Roux et al., 2005). The strength and specificity of the binding to gangliosides are therefore primary determinants of the kinetics of internalization and endocytic sorting of TeNT H_C and CTB.

In conclusion, we have shown that TeNT H_C internalization occurs via a specialized clathrin-dependent pathway, which is distinct from SV endocytosis and is preceded by a lateral sorting from its lipid raft–associated ligand GD1b. As for transferrin, TeNT H_C uptake relies on a nonredundant function of AP-2. However, transferrin endocytosis is dependent on epsin1, whereas TeNT H_C uptake is not, and may result in targeting of TeNT to neutral long-range transport compartments (Lalli et al., 2003a; Bohnert and Schiavo, 2005). These findings indicate that clathrin adaptors are assembled in a cargo-selective manner to drive the internalization of plasma membrane proteins and their ligands (Owen et al., 2004; Lakadamyali et al., 2006). This process has, in turn, the power to generate different populations of early endosomes, which have different targeting determinants and fates within the cell.

Materials and methods

Reagents

Chemicals were obtained from Sigma-Aldrich, BDH Chemicals Ltd., or Invitrogen, unless otherwise stated. Sulfo-NHS-SS-biotin and EZ-link–activated maleimide-HRP were purchased from Pierce Chemical Co. Antibodies 9E10, X22, and 12CA5 were obtained from the Cancer Research UK antibody facility, antibody 69.1 was purchased from Synaptic Systems, and the antibody against the C-terminus of SNAP-25 was a gift from O. Rossetto (University of Padova, Padova, Italy). The epsin1 antibody was a gift from L. Traub (University of Pittsburgh, Pittsburgh, PA). The IgG3 mouse monoclonal antibody MOG1 reacts with 8 M), and GD2, but not with GT1b, GQ1b, or GD3 (Boffey et–GD1b (Kd = 10 al., 2005). Plasmids encoding dynamin^{k44A}, epsin1$^{R63L\ H73L}$, and AP180 C-terminal mutants were a gift from H. McMahon (Laboratory of Molecular Biology, Cambridge, UK), AP-2 $\mu2^{T156A}$ was a gift from E. Smythe, and GFP-CLC was a gift from L. Greene

(National Institutes of Health, Bethesda, MD). TeNT HC was labeled with Alexa Fluor–maleimides (Lalli and Schiavo, 2002) or biotin, according to the manufacturers' instructions, followed by dialysis against PBS.

Protein labeling

To couple TeNT H_C to HRP, 10 nmol of cysteine-tagged TeNT H_C were incubated with 5 mM EDTA and 6.5 mg EZ-link–activated maleimide-HRP in PBS overnight at 4°C. The conjugate was purified first on ConA–Sepharose (GE Healthcare) and eluted with 0.25 M α-methylmannoside in 10 mM sodium phosphate, pH 7.2. HRP–TeNT H_C was bound to NiNTA-agarose (QIAGEN) and eluted in 20 mM Hepes-NaOH, pH 7.4, 150 mM NaCl, and 500 mM imidazole. Samples containing HRP–TeNT H_C were pooled and dialyzed against PBS. To double label TeNT H_C with an Alexa Fluor dye and HRP, fluorophore labeling was performed first, according to the manufacturer's instructions, using half of the recommended amount of dye and without the addition of glutathione to stop the reaction. Alexa Fluor–labeled TeNT H_C was dialyzed against PBS to remove the excess dye before HRP-conjugation.

Microinjection and internalization assay

MN cultures were prepared and maintained in culture as previously described (Bohnert and Schiavo, 2005). Cells were injected with 0.05 mg/ml of plasmid between 4 and 7 d in vitro. In cases of microinjection of multiple plasmids (e.g., the pTRE-μ2 T156A plasmid that requires a transactivator ptTA for expression; CLONTECH Laboratories, Inc.), 0.04 mg/ml of each construct were mixed before injection. MNs were incubated with 15–20 nM TeNT H_C and then either biotinylated or Alexa Fluor–labeled for 30 min at 37°C. In selected experiments, 20 μg/ml Alexa Fluor 594–transferrin, 10 ng/ml Alexa Fluor 555–CTB, or 0.2 mg/ml tetramethylrhodamine dextran (mol wt 3,000) were mixed with TeNT H_C before addition to the cells. 60 mM KCl was added to the medium just before addition of the ligands to test the effects of depolarization.

In experiments where MNs were pretreated with P4 or P4-scrambled peptide (Marks and McMahon, 1998), 50 μM of peptide was added to the medium at 37°C for 2 h before incubation with 20 nM Alexa Fluor 488–TeNT H_C and 0.2 mg/ml tetramethylrhodamine dextran.

For MESNA treatment, MNs were cooled on ice and then incubated three times for 15 min with 15 mM of ice-cold MESNA in neurobasal medium (Invitrogen), pH 8.3. Cells were washed three times in neurobasal medium and once in PBS, and then fixed.

To test the effect of SV exo/endocytosis on TeNT H_C uptake, MNs were seeded on 13-mm coverslips. At 6 d in vitro, MNs in two wells were incubated with 15 nM BoNT/A and 2 nM BoNT/D for 22 h at 37°C, while control wells were left untreated. Coverslips from treated and untreated wells were then transferred into a new dish and incubated with 20 nM b-TeNT H_C for a further 30 min at 37°C before treatment with MESNA on ice, fixing, and processing as described in the following paragraph. The remaining cells from each well were washed in PBS, scraped, centrifuged, and then resuspended in SDS sample buffer. Proteins were analyzed by Western blotting using standard procedures. Antibodies were used as follows: anti–VAMP-2 (69.1), 1:500; anti–SNAP-25, 1:1,000; anti-actin (AC-40), 1:1,000; and HRP-conjugated secondary antibodies (GE Healthcare), 1:1,000.

Immunofluorescence and confocal microscopy

Cells were fixed in 4% PFA and 20% sucrose in PBS for 15 min at room temperature, permeabilized with 0.1% Triton X-100 in PBS for 5 min, blocked in 2% BSA, 10% normal goat serum, and 0.25% fish skin gelatin in PBS for 30 min, and then incubated with the relevant antibodies (anti–VAMP-2 [69.1], 1:300; anti–SNAP-25, 1:300 [Washbourne et al., 1997]; anti-HA [12CA5], 1:1,000; anti-Myc [9E10], 1:250; secondary antibodies, 1:500; or streptavidin 1:500) for 30 min in blocking solution. Cells were mounted in Mowiol-488 and imaged using a LSM 510 laser scanning confocal microscope equipped with a 63×, 1.4 NA, Plan Apochromat oil-immersion objective (both Carl Zeiss MicroImaging, Inc.). Images were processed using LSM 510 software. Images showing GFP-CLC and TeNT H_C colocalization were taken on living cells at 37°C using a laser scanning confocal microscope (IX70; Olympus) equipped with a 60×, 1.2 W, UPlan Apochromat oil-immersion objective and an environmental chamber. Images were captured using the Ultraview Imaging Suite Version 5.5 software (Perkin Elmer) and processed using AQM Advance 6 Kinetic Acquisition Manager software (Kinetic Imaging).

EM

MNs grown on glass coverslips were incubated with 80 nM HRP–TeNT H_C and/or with 10 μg/ml MOG-1 antibody in serum-free neurobasal medium for 45 min at 4°C. Cells were then washed and chased in prewarmed medium at different temperatures for the indicated time. When appropriate, cells were incubated with a 10-nm gold-conjugated anti–mouse antibody (British Biocell International) on ice for additional 30 min and washed before chase in medium alone. Cells were then fixed with 2% PFA and 1.5% glutaraldehyde in 100 mM sodium cacodylate, pH 7.5, for 15 min and treated with DAB (0.75 mg/ml in 50 mM Tris-HCl, pH 7.4) and 0.02% H_2O_2 to cross-link HRP. Samples were postfixed and embedded in Epon as previously described (Stinchcombe et al., 1995). MNs were then sectioned en face, and 60-nm sections stained with lead citrate were viewed in an electron microscope (CM12; Philips).

For whole mounts, MNs were treated as in the pervious paragraph, but instead of being permeabilized with digitonin, they were extracted with 1% Triton X-100 in PBS containing 1 mM $MgCl_2$ and 0.1 mM $CaCl_2$ for 10 min at 5°C. After gold labeling, samples were fixed in 4% glutaraldehyde and 1% osmium, dehydrated, and critical-point dried before being prepared for carbon replicas (Hopkins, 1985).

For EM of microinjected cells, MNs were seeded on CELLocate glass-gridded coverslips (Eppendorf). A plasmid encoding ssHRP-KDEL (Connolly et al., 1994) was used as an injection marker. 26 h later, cells were treated with HRP–TeNT H_C and then with DAB, as described in the previous paragraphs. Alternatively, coverslips were incubated with 20 μg/ml human transferrin-HRP (Hopkins et al., 2000) after a 15-min preincubation at 37°C for in serum-free neurobasal medium. After fixation and embedding in Epon, ultrathin sections were cut from the grid area containing the microinjected cells and imaged by EM.

For immunolabeling, samples were incubated with DAB in 50 mM Tris-HCl, 110 mM NaCl, pH 7.4, or with ascorbic acid buffer (20 mM Hepes-NaOH, 70 mM NaCl, and 50 mM ascorbic acid, pH 7.0) at 5°C for 30 min after treatment with HRP–TeNT H_C and chased in medium. Cells were then permeabilized with 40 ng/ml digitonin in permeabilization buffer (25 mM Hepes-KOH, 38 mM aspartate, 38 mM glutamate, 38 mM gluconate, 2.5 mM $MgCl_2$, and 2 mM EGTA, pH 7.2), fixed in 2% PFA, quenched with 50 mM glycine, and blocked with 1% BSA before treatment with primary antibody in PBS containing 1% BSA for 60 min at room temperature. To enhance the signal, intermediate species-specific antibodies were used. MNs were washed and incubated with an appropriate 10-nm gold-labeled secondary antibody (British Biocell International) in 2% BSA and 2% FCS in PBS for 45 min at room temperature. After washing, cells were fixed and processed for conventional EM. In double- and triple-label experiments, MNs were incubated with 80 nM HRP–TeNT H_C or with 20 μg/ml transferrin-HRP together with TeNT H_C directly conjugated to 10-nm gold particles (as described by Odorizzi et al., 1996) in serum-free neurobasal medium for 45 min at 4°C. Cells were washed and shifted to 12 or 20°C before incubation with DAB/H_2O_2.

Online supplemental material

Fig. S1 shows biotinylated TeNT H_C as a probe to study membrane trafficking in MNs. Fig. S2 shows characterization of HRP–TeNT H_C. Fig. S3 shows that binding of TeNT H_C to MNs can be competed by preincubation with a specific anti-GD1b antibody. Fig. S4 shows distribution of TeNT H_C, epsin1, and transferrin in the endocytic pathway of MNs. Fig. S5 shows that overexpression of epsin1$^{R63L\ H73L}$ does not lead to AP-2 aggregation in spinal cord cells. Online supplemental material is available at http://www.jcb.org/cgi/content/full/jcb.200508170/DC1.

We are thankful to S. Tooze, A. Behrens, and members of the Molecular Neuropathobiology laboratory for critical reading of the manuscript.

This work was supported by Cancer Research UK (K. Deinhardt and G. Schiavo), Wellcome Trust 060349 (H.J. Willison), and the Medical Research Council (O. Berninghausen and C.R. Hopkins).

Submitted: 25 August 2005
Accepted: 6 July 2006

References

Abrami, L., S. Liu, P. Cosson, S.H. Leppla, and F.G. van der Goot. 2003. Anthrax toxin triggers endocytosis of its receptor via a lipid raft-mediated clathrin-dependent process. *J. Cell Biol.* 160:321–328.

Aquino, D.A., M.A. Bisby, and R.W. Ledeen. 1985. Retrograde axonal transport of gangliosides and glycoproteins in the motoneurons of rat sciatic nerve. *J. Neurochem.* 45:1262–1267.

Blanpied, T.A., D.B. Scott, and M.D. Ehlers. 2002. Dynamics and regulation of clathrin coats at specialized endocytic zones of dendrites and spines. *Neuron*. 36:435–449.

Boffey, J., M. Odaka, D. Nicoll, E.R. Wagner, K. Townson, T. Bowes, J. Conner, K. Furukawa, and H.J. Willison. 2005. Characterisation of the immunoglobulin variable region gene usage encoding the murine anti-ganglioside antibody repertoire. *J. Neuroimmunol.* 165:92–103.

Bohnert, S., and G. Schiavo. 2005. Tetanus toxin is transported in a novel neuronal compartment characterized by a specialized pH regulation. *J. Biol. Chem.* 280:42336–42344.

Chen, H., and P. De Camilli. 2005. The association of epsin with ubiquitinated cargo along the endocytic pathway is negatively regulated by its interaction with clathrin. *Proc. Natl. Acad. Sci. USA*. 102:2766–2771.

Conner, S.D., and S.L. Schmid. 2003. Differential requirements for AP-2 in clathrin-mediated endocytosis. *J. Cell Biol.* 162:773–779.

Conner, S.D., S.L. Schmid, M. Masserini, P. Palestini, and M. Pitto. 2003. Regulated portals of entry into the cell. *Nature*. 422:37–44.

Connolly, C.N., C.E. Futter, A. Gibson, C.R. Hopkins, and D.F. Cutler. 1994. Transport into and out of the Golgi complex studied by transfecting cells with cDNAs encoding horseradish peroxidase. *J. Cell Biol.* 127:641–652.

Damke, H., T. Baba, D.E. Warnock, and S.L. Schmid. 1994. Induction of mutant dynamin specifically blocks endocytic coated vesicle formation. *J. Cell Biol.* 127:915–934.

Deinhardt, K., and G. Schiavo. 2005. Endocytosis and retrograde axonal traffic in motor neurons. *Biochem. Soc. Symp.* 72:139–150.

Ehrlich, M., W. Boll, A. Van Oijen, R. Hariharan, K. Chandran, M.L. Nibert, and T. Kirchhausen. 2004. Endocytosis by random initiation and stabilization of clathrin-coated pits. *Cell*. 118:591–605.

Ford, M.G., I.G. Mills, B.J. Peter, Y. Vallis, G.J. Praefcke, P.R. Evans, and H.T. McMahon. 2002. Curvature of clathrin-coated pits driven by epsin. *Nature*. 419:361–366.

Ford, M.G., B.M. Pearse, M.K. Higgins, Y. Vallis, D.J. Owen, A. Gibson, C.R. Hopkins, P.R. Evans, and H.T. McMahon. 2001. Simultaneous binding of PtdIns(4,5)P2 and clathrin by AP180 in the nucleation of clathrin lattices on membranes. *Science*. 291:1051–1055.

Glebov, O.O., N.A. Bright, and B.J. Nichols. 2006. Flotillin-1 defines a clathrin-independent endocytic pathway in mammalian cells. *Nat. Cell Biol.* 8:46–54.

Habermann, E., and F. Dreyer. 1986. Clostridial neurotoxins: handling and action at the cellular and molecular level. *Curr. Top. Microbiol. Immunol.* 129:93–179.

Harding, C., J. Heuser, and P. Stahl. 1983. Receptor-mediated endocytosis of transferrin and recycling of the transferrin receptor in rat reticulocytes. *J. Cell Biol.* 97:329–339.

Herreros, J., T. Ng, and G. Schiavo. 2001. Lipid rafts act as specialized domains for tetanus toxin binding and internalization into neurons. *Mol. Biol. Cell*. 12:2947–2960.

Hinrichsen, L., J. Harborth, L. Andrees, K. Weber, and E.J. Ungewickell. 2003. Effect of clathrin heavy chain- and alpha-adaptin-specific small inhibitory RNAs on endocytic accessory proteins and receptor trafficking in HeLa cells. *J. Biol. Chem.* 278:45160–45170.

Hopkins, C.R. 1985. The appearance and internalization of transferrin receptors at the margins of spreading human tumor cells. *Cell*. 40:199–208.

Hopkins, C., A. Gibson, J. Stinchcombe, and C. Futter. 2000. Chimeric molecules employing horseradish peroxidase as reporter enzyme for protein localization in the electron microscope. *Methods Enzymol.* 327:35–45.

Huang, F., A. Khvorova, W. Marshall, and A. Sorkin. 2004. Analysis of clathrin-mediated endocytosis of epidermal growth factor receptor by RNA interference. *J. Biol. Chem.* 279:16657–16661.

Humeau, Y., F. Doussau, N.J. Grant, and B. Poulain. 2000. How botulinum and tetanus neurotoxins block neurotransmitter release. *Biochimie*. 82:427–446.

Kirkham, M., A. Fujita, R. Chadda, S.J. Nixon, T.V. Kurzchalia, D.K. Sharma, R.E. Pagano, J.F. Hancock, S. Mayor, and R.G. Parton. 2005. Ultrastructural identification of uncoated caveolin-independent early endocytic vehicles. *J. Cell Biol.* 168:465–476.

Kitamura, M., K. Takamiya, S. Aizawa, and K. Furukawa. 1999. Gangliosides are the binding substances in neural cells for tetanus and botulinum toxins in mice. *Biochim. Biophys. Acta*. 1441:1–3.

Lakadamyali, M., M.J. Rust, and X. Zhuang. 2006. Ligands for clathrin-mediated endocytosis are differentially sorted into distinct populations of early endosomes. *Cell*. 124:997–1009.

Lalli, G., and G. Schiavo. 2002. Analysis of retrograde transport in motor neurons reveals common endocytic carriers for tetanus toxin and neurotrophin receptor p75NTR. *J. Cell Biol.* 156:233–239.

Lalli, G., S. Bohnert, K. Deinhardt, C. Verastegui, and G. Schiavo. 2003a. The journey of tetanus and botulinum neurotoxins in neurons. *Trends Microbiol.* 11:431–437.

Lalli, G., S. Gschmeissner, and G. Schiavo. 2003b. Myosin Va and microtubule-based motors are required for fast axonal retrograde transport of tetanus toxin in motor neurons. *J. Cell Sci.* 116:4639–4650.

Lamaze, C., A. Dujeancourt, T. Baba, C.G. Lo, A. Benmerah, and A. Dautry-Varsat. 2001. Interleukin 2 receptors and detergent-resistant membrane domains define a clathrin-independent endocytic pathway. *Mol. Cell*. 7:661–671.

Le Roy, C., and J.L. Wrana. 2005. Clathrin- and non-clathrin-mediated endocytic regulation of cell signalling. *Nat. Rev. Mol. Cell Biol.* 6:112–126.

Marks, B., and H.T. McMahon. 1998. Calcium triggers calcineurin-dependent synaptic vesicle recycling in mammalian nerve terminals. *Curr. Biol.* 8:740–749.

Massol, R.H., J.E. Larsen, Y. Fujinaga, W.I. Lencer, and T. Kirchhausen. 2004. Cholera toxin toxicity does not require functional Arf6- and dynamin-dependent endocytic pathways. *Mol. Biol. Cell*. 15:3631–3641.

Matteoli, M., C. Verderio, O. Rossetto, N. Iezzi, S. Coco, G. Schiavo, and C. Montecucco. 1996. Synaptic vesicle endocytosis mediates the entry of tetanus neurotoxin into hippocampal neurons. *Proc. Natl. Acad. Sci. USA*. 93:13310–13315.

Miana-Mena, F.J., S. Roux, J.C. Benichou, R. Osta, and P. Brulet. 2002. Neuronal activity-dependent membrane traffic at the neuromuscular junction. *Proc. Natl. Acad. Sci. USA*. 99:3234–3239.

Miller, F.D., and D.R. Kaplan. 2001. On Trk for retrograde signaling. *Neuron*. 32:767–770.

Montecucco, C., O. Rossetto, and G. Schiavo. 2004. Presynaptic receptor arrays for clostridial neurotoxins. *Trends Microbiol.* 12:442–446.

Montesano, R., J. Roth, A. Robert, and L. Orci. 1982. Non-coated membrane invaginations are involved in binding and internalization of cholera and tetanus toxin. *Nature*. 296:651–653.

Motley, A., N.A. Bright, M.N. Seaman, and M.S. Robinson. 2003. Clathrin-mediated endocytosis in AP-2-depleted cells. *J. Cell Biol.* 162:909–918.

Munro, P., H. Kojima, J.L. Dupont, J.L. Bossu, B. Poulain, and P. Boquet. 2001. High sensitivity of mouse neuronal cells to tetanus toxin requires a GPI-anchored protein. *Biochem. Biophys. Res. Commun.* 289:623–629.

Murthy, V.N., and P. De Camilli. 2003. Cell biology of the presynaptic terminal. *Annu. Rev. Neurosci.* 26:701–728.

Nesterov, A., R.E. Carter, T. Sorkina, G.N. Gill, and A. Sorkin. 1999. Inhibition of the receptor-binding function of clathrin adaptor protein AP-2 by dominant-negative mutant mu2 subunit and its effects on endocytosis. *EMBO J.* 18:2489–2499.

Nichols, B.J. 2003. GM1-containing lipid rafts are depleted within clathrin-coated pits. *Curr. Biol.* 13:686–690.

Odorizzi, G., A. Pearse, D. Domingo, I.S. Trowbridge, and C.R. Hopkins. 1996. Apical and basolateral endosomes of MDCK cells are interconnected and contain a polarized sorting mechanism. *J. Cell Biol.* 135:139–152.

Olusanya, O., P.D. Andrews, J.R. Swedlow, and E. Smythe. 2001. Phosphorylation of threonine 156 of the mu2 subunit of the AP2 complex is essential for endocytosis in vitro and in vivo. *Curr. Biol.* 11:896–900.

Owen, D.J., B.M. Collins, and P.R. Evans. 2004. Adaptors for clathrin coats: structure and function. *Annu. Rev. Cell Dev. Biol.* 20:153–191.

Parton, R.G., and A.A. Richards. 2003. Lipid rafts and caveolae as portals for endocytosis: new insights and common mechanisms. *Traffic*. 4:724–738.

Parton, R.G., C.D. Ockleford, and D.R. Critchley. 1987. A study of the mechanism of internalisation of tetanus toxin by primary mouse spinal cord cultures. *J. Neurochem.* 49:1057–1068.

Roux, S., C. Colasante, C. Saint Cloment, J. Barbier, T. Curie, E. Girard, J. Molgo, and P. Brulet. 2005. Internalization of a GFP-tetanus toxin C-terminal fragment fusion protein at mature mouse neuromuscular junctions. *Mol. Cell. Neurosci.* 30:79–89.

Rummel, A., S. Bade, J. Alves, H. Bigalke, and T. Binz. 2003. Two carbohydrate binding sites in the H(CC)-domain of tetanus neurotoxin are required for toxicity. *J. Mol. Biol.* 326:835–847.

Sabharanjak, S., P. Sharma, R.G. Parton, and S. Mayor. 2002. GPI-anchored proteins are delivered to recycling endosomes via a distinct cdc42-regulated, clathrin-independent pinocytic pathway. *Dev. Cell*. 2:411–423.

Saint-Pol, A., B. Yelamos, M. Amessou, I.G. Mills, M. Dugast, D. Tenza, P. Schu, C. Antony, H.T. McMahon, C. Lamaze, and L. Johannes. 2004. Clathrin adaptor epsinR is required for retrograde sorting on early endosomal membranes. *Dev. Cell*. 6:525–538.

Sandvig, K., and B. van Deurs. 2002. Membrane traffic exploited by protein toxins. *Annu. Rev. Cell Dev. Biol.* 18:1–24.

Schmid, S.L., and E. Smythe. 1991. Stage-specific assays for coated pit formation and coated vesicle budding in vitro. *J. Cell Biol.* 114:869–880.

Schwab, M.E., and H. Thoenen. 1978. Selective binding, uptake, and retrograde transport of tetanus toxin by nerve terminals in the rat iris. An electron microscope study using colloidal gold as a tracer. *J. Cell Biol.* 77:1–13.

Shogomori, H., and A.H. Futerman. 2001. Cholera toxin is found in detergent-insoluble rafts/domains at the cell surface of hippocampal neurons but is internalized via a raft-independent mechanism. *J. Biol. Chem.* 276:9182–9188.

Sigismund, S., T. Woelk, C. Puri, E. Maspero, C. Tacchetti, P. Transidico, P.P. Di Fiore, and S. Polo. 2005. Clathrin-independent endocytosis of ubiquitinated cargos. *Proc. Natl. Acad. Sci. USA*. 102:2760–2765.

Signoret, N., L. Hewlett, S. Wavre, A. Pelchen-Matthews, M. Oppermann, and M. Marsh. 2005. Agonist-induced endocytosis of CC chemokine receptor 5 is clathrin dependent. *Mol. Biol. Cell*. 16:902–917.

Stinchcombe, J.C., H. Nomoto, D.F. Cutler, and C.R. Hopkins. 1995. Anterograde and retrograde traffic between the rough endoplasmic reticulum and the Golgi complex. *J. Cell Biol.* 131:1387–1401.

Stoorvogel, W. 1998. Analysis of the endocytic system by using horseradish peroxidase. *Trends Cell Biol.* 8:503–505.

Sunyach, C., A. Jen, J. Deng, K.T. Fitzgerald, Y. Frobert, J. Grassi, M.W. McCaffrey, and R. Morris. 2003. The mechanism of internalization of glycosylphosphatidylinositol-anchored prion protein. *EMBO J.* 22:3591–3601.

Torgersen, M.L., G. Skretting, B. van Deurs, and K. Sandvig. 2001. Internalization of cholera toxin by different endocytic mechanisms. *J. Cell Sci.* 114:3737–3747.

Venkatesan, S., J.J. Rose, R. Lodge, P.M. Murphy, and J.F. Foley. 2003. Distinct mechanisms of agonist-induced endocytosis for human chemokine receptors CCR5 and CXCR4. *Mol. Biol. Cell*. 14:3305–3324.

Washbourne, P., R. Pellizzari, G. Baldini, M.C. Wilson, and C. Montecucco. 1997. Botulinum neurotoxin types A and E require the SNARE motif in SNAP-25 for proteolysis. *FEBS Lett.* 418:1–5.